8 Oct 2001

FY 2001 Annual Report
N00014-99-1-0313

Nanoscale coherence near defects: Superconductivity, spin ordering, and their coexistence

PI Name: **Michael E. Flatté**
Address: **Department of Physics and Astronomy, University of Iowa, Iowa City, IA 52242**
Phone: **(319) 335-0201**
Fax: **(319) 353-1115**
Email: **michael-flatte@uiowa.edu**
Web site: **http://ostc.physics.uiowa.edu/~flatte**

Long-term goals:

This theoretical effort focuses on understanding and calculating the effects of impurities on the properties of high-temperature superconducting interfaces, particularly those of interest in tunneling and microwave devices. A particular emphasis is placed on correlating theoretical calculations with experimental information, and developing towards a better understanding of the properties of the technologically important material $YBa_2Cu_3O_{7+\delta}$. Built on theoretical tools developed during the current and previous ONR grants, self-consistent, accurate calculations are underway of the effects of magnetic and nonmagnetic impurities on microwave and tunneling properties of importance in devices.

Objectives:

To work with experimentalists to identify the signatures of particular impurities in junction performance.

To identify the characteristic features of noise in tunnel junctions, and how noise can be used to probe the time-dependent dynamics of a fluctuating order parameter.

To calculate the effect of impurities or grain boundaries on supercurrent transport through a junction with arbitrary transparency.

To calculate the effects of strong dynamic impurities on the nearby electronic structure, as well as on junction behavior, dielectric loss, and magnetic penetration depth.

To improve the bulk band structures used for high-temperature superconductors to those that reflect the best electronic structure models currently available.

To investigate defect and interface phenomena involving new materials.

Approach:

The influence of defects is calculated using a self-consistent Green's function approach (Koster-Slater technique) pioneered by the P.I. for impurity calculations in superconductors[1]. This technique will be generalized to deal with time-dependent (fluctuating) order parameters and also for application to dynamic impurities. More detailed band structures will be obtained from multiband tight-binding parametrizations of full density-functional-theory calculations, as well as parametrizations of experimental probes of band structure such as angle-resolved photoemission.

I have been fortunate enough to recruit an excellent postdoc, Dr. Jian-Ming Tang, who did his Ph.D. work with Prof. Thouless at U. Washington. Dr. Tang has extensive experience in the properties of vortices in novel superconductors, and is highly motivated to calculate the properties of defects in superconductors as well as their microwave properties. Dr. Tang is also very gifted in numerical computation. I am very excited now that Dr. Tang has joined my effort, for I expect the work will now proceed much more rapidly.

Work completed:

The P.I. has performed improved his calculations of the properties of nickel and zinc impurities in the high-temperature superconductor $Bi_2Sr_2CaCu_2O_{8+\delta}$ (BSCCO) and compared with the recent observations of J. C. Davis at U. C. Berkeley. The P.I. has suggested the use of Ni to probe superconducting coherence in the inhomogeneous superconducting state on the surface of BSCCO – this experiment has since been performed, indicating inhomogeneity in the superconducting character of BSCCO. The P.I. has also added to his quantitative calculations the energy-dependent linewidth observed experimentally in a variety of experiments, and also introduced the bilayer splitting with *d*-orbital character which has been seen in ARPES. In the process the P.I. has dramatically improved the quality of the connection between electronic structure measurements from ARPES and tunneling. He has subsequently predicted the amplitude of impurity resonances that should be visible in the lower bilayer of BSCCO. He has extracted some impurity parameters for $YBa_2Cu_3O_{7+d}$ (YBCO) and calculations of impurity structure in YBCO are underway. The P.I. has also completed much of the initial theory picture for noise in tunneling due to fluctuating order parameters – quantitative calculations will be underway very soon.

Results:

Nanoscale inhomogeneity and the use of Ni as a probe of local superconductivity:

The P.I. has previously proposed that quasiparticle resonances near an impurity atom could be used as a sensitive probe of local electronic properties, and particularly whether the local environment near the impurity were superconducting or not [see P.I. publications 1 and 2]. The behavior of the quasiparticle resonance near Zn was suggested to be indicative of local destruction of superconductivity, whereas that near Ni as evidence of well-behaved superconducting regions.

Recently Davis' group at UC Berkeley has taken this suggestion to heart and used Ni to probe the superconducting nature of BSCCO surfaces. Having previously discovered that these surfaces were strongly inhomogeneous, Davis' group has now demonstrated that there are no Ni resonances in certain identifiable regions of the surface (those with a gap exceeding 45 meV). As the Ni atoms are distributed randomly in the superconductor, the implication is the electronic structure of these regions does not support quasiparticle resonances.

This is very strong evidence that these regions are not superconducting, and also that they may not have the ordinary robust quasiparticles of a Fermi liquid. The implications of this are legion – it provides clues to the origin of the peculiar pseudogap state, and suggests that the superconducting state can be understood as a percolative state of superconducting grains embedded in a non-superconducting background. Such an understanding is critical to understand the nature and lifetime of quasiparticles in the superconducting state, key to microwave loss mechanisms. This use of Ni as a spectroscopic probe of the *local* degree of superconductivity can now be expected to be applied experimentally to other defects in the superconducting material: vacancies, vortices, step edges, and other impurity atoms.

Further development in understanding impurities in YBCO is now important. If, as seems likely, Ni is a good probe of superconducting coherence in YBCO as well, then Ni should be used to probe the nature of superconductivity in the YBCO environment, including both the planes and the chains (and possibly in stripes as well).

Detailed probes of electronic structure

Models of the electronic structure of high-temperature superconductors are usually based on either ab-initio calculations or empirical parametrizations of photoemission data. The ab-initio calculations are notoriously inaccurate, predicting features in the electronic structure that are not observed (Bi-O pockets in BSCCO) and even getting the overall bandwidth wrong by a factor of two. Photoemission parametrizations should be more reliable, as they are based on direct experimental observation. The observations of nanoscale inhomogeneity, however, suggest concern about parametrizations extracted from photoemission measurements that were performed over a broad surface area.

For example, the use of photoemission parametrizations for the electronic structure and the superconducting energy gap yield tunneling spectra in BSCCO that generally have too many low-energy quasiparticles. They also yield spectra for Ni resonances that are too broad compared with experiment. Using the tunneling spectra measured in clean regions on BSCCO in conjunction with ARPES we are developing refined models of the electronic structure. These refined models also provide quasiparticle resonances in good agreement with experiment. (Fig. 1 shows tunneling calculations for the bulk material including bilayer splitting.)

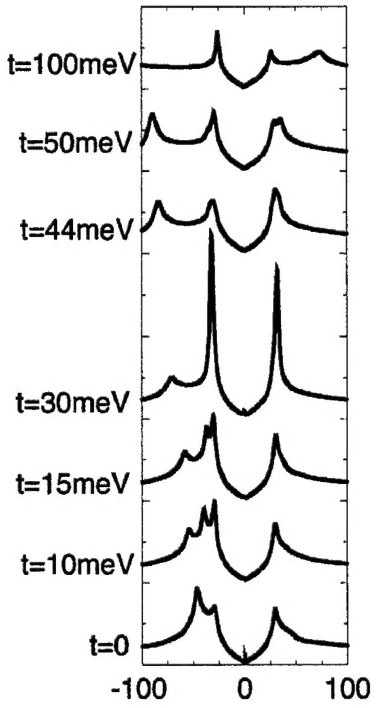

Figure 1: calculated tunneling spectra incorporating both the energy-dependent linewidth and a bilayer splitting of the functional form measured by ARPES. The magnitude of the energy-dependent linewidth and the bilayer splitting was determined by a best fit to tunneling (as ARPES had not measured for the specific doping in the tunneling experiment). These curves are far superior in agreement with tunneling experiment than any others obtained to date.

The key implications of these investigations are: (1) more accurate models of low-energy quasiparticles, of importance principally in microwave loss calculations, but also important for tunneling calculations, (2) the dependence of the impurity

Finally, motivated by photoemission observation of bilayer splitting in BSCCO, we have calculated the influence of bilayer splitting on low-energy quasiparticles and impurity resonances. We find that the low-energy quasiparticles are not altered significantly by bilayer splitting, and the impurity resonances are only slightly shifted in energy. An important result is that bilayer splitting itself does not split the impurity resonances (Fig. 2). We also find the amplitude of the "shadow" of an impurity atom in the next layer is dependent most strongly on the bilayer coupling.

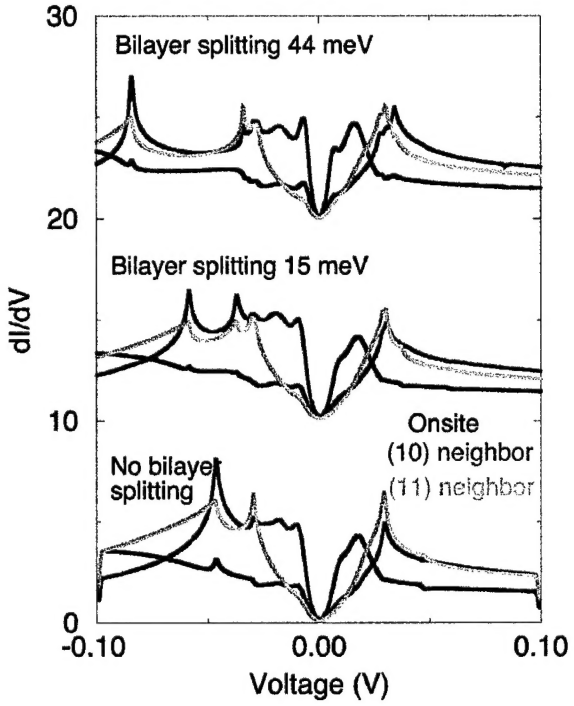

Figure 2: Calculated impurity resonances in the bilayer structure, with and without bilayer splitting. Shown are on-site (black), nearest neighbor (red), and next-nearest neighbor (green) spectra. A key observation is that the bilayer splitting does not dramatically change the impurity resonances, and in particular does not split them.

atom "shadow" in the other layer of a bilayer structure on the magnitude of the bilayer tunneling matrix element, of importance for c-axis tunneling, and (3) the suggestion that for low-energy quasiparticles a single-layer model is quite sufficient for accurate calculations of some microwave properties.

These quantitative improvements are also essential to develop an understanding appropriate for YBCO. Bilayer splitting in YBCO has now been measured, along with the energy-dependent linewidth. Finally, though c-axis conductivity measurements in YBCO the important matrix element for the coupling of the impurity atom in a plane to a Cu-O plane in the *next* unit cell along the c-axis is known. Curiously that matrix element squared is 12 times larger than the matrix element for Cu, indicating that these impurities dramatically affect the interplane tunneling matrix element in YBCO. This interplane tunneling matrix element is vital for making quantitative comparison with measurements near impurities in YBCO. The first such measurement was reported by Yeh recently. Yeh's results are important due to the technological importance of YBCO, even though the signal to noise is lower than for BSCCO, and the topography is not as sharp as BSCCO. It is likely that sharper results will be obtained soon by Yeh or others. For example, in the controlled termination MBE growths of YBCO by Eckstein (which will be examined by Yazdani), no doubt the properties of impurities exposed in a controlled termination will be investigated.

Preliminary Theory of Noise due to Order Parameter Fluctuations in STM Spectra

Several models of the electronic structure, particularly in YBCO, predict fluctuating order parameters that could be expected to produce noise in tunneling spectra. The P.I. argued in his proposal that if there was a fluctuating order parameter in a system, that it would cause the quasiparticle resonant peak coming from anomalous processes (electrons turning into holes and holes turning into electrons in the superconductor) to generate a peak in the noise spectrum at a frequency corresponding to $1/T_{fluc}$, where T_{fluc} is the typical fluctuation time.

Since then the P.I. has identified other characteristic features of noise and how they relate to the order parameter fluctuation spectrum. First, common models of the order parameter in high-temperature superconductors assume that the interesting structure is just in the momentum-space structure; they ignore the frequency dependence (which arises, e.g. in an Eliashberg calculation). Fluctuations, however, affect the order parameter differently depending on the frequency probed, and independent of the momentum structure. For example, in mean field theory the low-frequency order parameter is very strongly affected by fluctuations, but the high-frequency order parameter is not. The qualitative statement is that for frequencies lower than $1/T_{fluc}$, the order parameter is largely averaged away, whereas for frequencies higher than $1/T_{fluc}$ the order parameter is largely unaffected. This may explain puzzling discrepancies between theory and experiment on the number of low-energy quasiparticles seen in YBCO – it may be the case that the effective order parameter is negligible at low energies, but large at high energies (thus one would still see a gap structure). The P.I. is in the process of calculating the influence of this effect on impurity resonances. Another implication of this analysis is that the noise

spectrum is expected to be very dependent on the tunnel voltage (energy of injected electron or hole).

Impact/Applications:

An improved understanding of single-impurity properties will allow for an improved understanding of macroscopic quantities which depend on many impurities. These include, in addition to junction performance, the magnetic penetration depth and dielectric loss, which are important for superconductor-based mixers. Calculations of magnetic penetration depth and dielectric loss using the single-impurity results of the P.I. are underway, so that he can "close the loop" with device properties.

Transitions: None

Related Projects:

The experimental programs of J. C. Davis at UC Berkeley and J. Eckstein/A. Yazdani at UIUC are the most closely related projects. Connections to projects focusing on understanding the origin of dielectric loss, such as S. Sridhar's at Northeastern, will be improved over the next year as calculations of these properties are performed.

Publications:

Publications Appeared:

1) "Nickel probes superconductivity", Michael E. Flatté, Nature (news and views) **411**, 901 (2001).

2) "Quasiparticle resonant states as a probe of short-range electronic structure and Andreév coherence", Michael E. Flatté, *Physical Review B* **61**, R14920 (2000).

3) "The Local Spectrum of a Superconductor as a Probe of the Interaction Between Magnetic Impurities", Michael E. Flatté and David. E. Reynolds *Physical Review B*, **61**, 14810 (2000).

Invited Talks:

1) "Impurity resonances as local probes of superconductivity", Defects in Correlated Electron Systems (DICES), Dresden, Germany, July 24, 2001.

2) "Local properties of magnetic impurities in high-T_c superconductors", Seminar, Stanford University, May 3, 2001.

Patents: None.

the predicted three-way correlation between sensitivity, light and colour.

Cause and effect, though, are not clear. As Boughman says, male coloration could have evolved to match female spectral sensitivity, as suggested by one hypothesis (the 'sensory exploitation' hypothesis[11]). Or both colour and sensitivity could have evolved independently to match ambient light levels. A final possibility, which Boughman does not mention, is that the contrasting colours could initially have evolved in the males, with females then developing their spectral sensitivity to match the signal. Only an analysis of evolutionary relationships could distinguish between these possibilities.

Does divergence in male traits and female preferences contribute to reproductive isolation? In this case it does. Boughman found that females that are more sensitive to red also prefer redder males within their population, and that the probability of spawning between populations is related to the degree of divergence in male redness and female preference for red. Unlike in some other studies of sticklebacks[10], however, we do not know whether the mate preferences between populations are due to overall brightness, to true colour alone, or to the contrast of colour with the background or with other body parts.

Much of the study of speciation can be distilled into trying to understand how reproductive isolation happens[12]. As Boughman has shown, her approach can provide detailed knowledge of how reproductive isolation comes about in sticklebacks. Future studies might tackle the intriguing subject of the neural and genetic mechanisms underlying the changes in spectral sensitivity that mediate this female preference. Is preference determined by the absorption spectrum of the photopigment that is sensitive to long wavelengths[13]? If so, one might be able to identify changes in the structure of the pigment molecules that account for such differences, and thus be able to identify one of the genes that contribute to speciation in sticklebacks (as has been claimed for the fruitfly *Drosophila*[14]).

Alternatively, the differences in female preference could be related to the number of long-wavelength-sensitive cones in the retina, or to the proportion of spectrally opponent neurons in the visual system. Furthermore, mathematical models of how visual scenes are analysed, some of which have been applied to sticklebacks[10], could offer further insights into why not all females see red in the same way. All in all, sticklebacks may be outstanding subjects for investigating the biology of speciation in general. ■

Michael J. Ryan is in the Section of Integrative Biology, University of Texas, Austin, Texas 78712-1064, USA.
e-mail: mryan@mail.utexas.edu

1. Boughman, J. W. *Nature* **411**, 944–948 (2001).
2. Cronin, H. *The Ant and the Peacock* (Cambridge Univ. Press, 1991).
3. West-Eberhard, M. J. *Proc. Am. Phil. Soc.* **123**, 222–234 (1979).
4. Lande, R. *Proc. Natl Acad. Sci. USA* **78**, 3721–3725 (1981).
5. Endler, J. A. *Am. Nat.* **131**, S125–S153 (1992).
6. Marchetti, K. *Nature* **362**, 149–152 (1993).
7. McPhail, J. D. *Can. J. Zool.* **71**, 515–523 (1995).
8. Rundle, H. D., Nagel, L., Boughman, J. W. & Schluter, D. *Science* **287**, 306–308 (2000).
9. Tinbergen, N. in *Psychobiology, the Biological Bases of Behavior: Readings from Scientific American* 5–9 (Freeman, San Francisco, 1952).
10. Baube, C. L., Rowland, W. J. & Fowler, J. B. *Behaviour* **132**, 979–996 (1995).
11. Ryan, M. J. *Oxford Surv. Evol. Biol.* **7**, 157–195 (1990).
12. Coyne, J. A. & Orr, H. A. *Phil. Trans. R. Soc. Lond. B* **353**, 287–305 (1998).
13. Yokoyama, S. & Yokoyama, R. *Annu. Rev. Ecol. Syst.* **27**, 543–567 (1996).
14. Ting, C.-T., Tsaur, S.-C. & Wu, C.-I. *Proc. Natl Acad. Sci. USA* **97**, 5313–5316 (2000).

Condensed-matter physics

Nickel probes superconductivity

Michael E. Flatté

Magnetism usually destroys superconductivity, but a magnetic nickel atom inserted into a high-temperature superconductor has surprisingly little effect on its local environment.

The unusual properties of superconductors arise from the coherent behaviour of electrons when they flow together in pairs. Two key properties for electrons in a superconductor are their negative charge, which normally keeps them apart, and their spin, which can be thought of as a tiny bar magnet, pointing either up or down. If electrons of opposite spin overcome their mutual repulsion they can form Cooper pairs and flow without resistance — the essence of superconductivity. One useful way of exploring the properties of a superconductor is to alter this pairing coherence.

Applying a magnetic field disrupts the pairing of electrons, and as a result, diminishes the energy required to break Cooper pairs, thereby reducing the 'transition temperature' at which the material becomes superconducting. A sufficiently large magnetic field can even disrupt pairing to the point where the material ceases to be superconducting. Adding a single magnetic atom to a superconductor creates a similar effect, although the perturbation to the superconductor is localized near the magnetic atom. On page 920 of this issue, Hudson *et al.*[1] describe the effect of adding a magnetic nickel atom to a high-temperature superconductor. Nickel weakly perturbs its local environment in the superconductor, suggesting that this impurity could be used as a non-invasive probe of superconducting behaviour on the nanoscale.

In a superconductor, pairing coherence occurs when a free electron 'grabs' an electron of opposite spin, forming a Cooper pair and leaving behind a positively charged 'hole' in the electron sea of the superconduc-

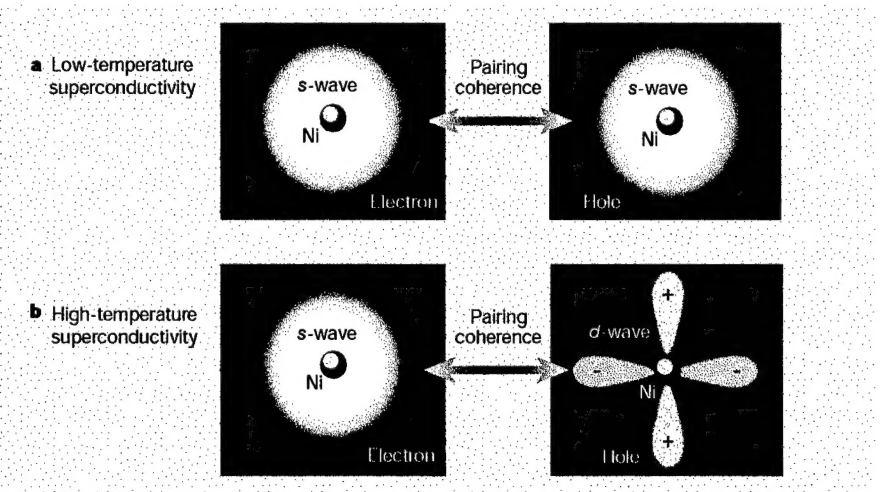

Figure 1 **Quasiparticles in a superconductor. An electron bound to an impurity atom, such as nickel (Ni), mixes with a hole, to form a low-energy Bogoliubov quasiparticle. a, In a conventional superconductor, like niobium, the symmetry of the wavefunction of the electron component and of the hole component are identical. They both have *s*-wave (spherical) symmetry. b, In a high-temperature superconductor, like the one studied by Hudson *et al.*[1], the electrons that form the Cooper pairs rapidly revolve around each other, to keep their distance and lower their mutual repulsion. The *d*-wave nature of their angular momentum is reflected in the *d*-wave symmetry of the hole component of the associated quasiparticle.**

tor. This mixture of the original electron and the hole left behind is known as a Bogoliubov quasiparticle. The nature of the Cooper pairs, and hence of Bogoliubov quasiparticles, is greatly different in high-temperature superconductors and conventional superconductors. In high-temperature superconductors the two electrons in a Cooper pair revolve around each other rapidly to increase their separation. This reduces the energy cost of having two negatively charged particles close together. Mutual revolution of electrons in a Cooper pair is labelled by angular momentum as *s*, *p* or *d*, just like electrons revolving around the nucleus of an atom. The rapid revolution of the electron pair also causes the Bogoliubov quasiparticles to have a peculiar shape. If the electron component of the quasiparticle is bound to a nickel atom, the hole component must rapidly revolve around the nickel atom, in a way that reflects the nature of the Cooper pairs[2] (Fig. 1). So in a low-temperature superconductor, the hole would have *s*-wave symmetry, whereas in a high-temperature superconductor it would have *d*-wave symmetry.

The nickel atom embedded in the high-temperature superconductor studied by Hudson *et al.*[1] does appear to attract electrons. The authors viewed the area around the nickel atom using a scanning tunnelling microscope (STM), which is sensitive to the density of electronic states near the impurity. They observe two new distinct quasiparticle energies near the nickel atom, corresponding to Bogoliubov quasiparticles with opposite spin. So the experiment of Hudson *et al.* is a direct observation of quasiparticles of distinct spin formed near an individual impurity atom. They have also separately observed the electron and hole components of each quasiparticle by changing the STM voltage from positive (in which an electron is inserted into the superconductor) to negative (in which a hole is inserted). The results directly confirm for the first time that the hole component has the expected *d*-wave symmetry of a high-temperature superconductor.

Hudson and colleagues' results suggest that the influence of a magnetic nickel atom on its local environment in a high-temperature superconductor is surprisingly weak, despite its strong effect on global properties, such as the superconducting transition temperature. For a conventional superconductor like niobium, embedded magnetic atoms also strongly suppress the transition temperature, and have a weak local effect when placed on the surface[3]. Other impurity atoms in high-temperature superconductors, such as non-magnetic zinc, have a similar effect to nickel on the transition temperature. But earlier measurements of quasiparticles near a zinc atom[4] showed dramatic distortions of the local environment. The zinc-associated quasiparticles also lacked any electron component. These differences suggest that near a zinc atom there may be additional electronic interactions that strongly reduce pairing coherence.

Many studies have shown that high-temperature superconductors doped with nickel behave differently from those doped with other atoms. But Hudson and colleagues' measurements show for the first time that impurity atoms can be present in high-temperature superconductors without dramatically destroying the superconductivity in their local surroundings. The authors suggest that their results have implications for understanding the pairing mechanism underlying high-temperature superconductivity — in particular, whether it has a magnetic origin. It is still too early to favour one mechanism over another, but the importance of their measurements goes beyond these immediate issues.

The focus of high-temperature superconductivity is shifting to the nanoscale, particularly to the effect of small structures in the superconductor on the formation of Cooper pairs. The properties of nickel make it an ideal tool for exploring nanoscale superconductivity. In medical technology, radioactive markers are attached to a molecule to track its motion; here, nickel atoms can be used as 'pairing markers' for inhomogeneous environments in a superconductor. If it is believed that the presence of a particular object in the superconductor, such as a zinc atom or a magnetic field line, destroys pairing coherence over a distance much longer than the atomic spacing, then nickel atoms could be 'seeded' in the vicinity of that object. Then, using STM techniques, any low-energy quasiparticles created near the nickel atom could be monitored for unusual behaviour.

Nickel atoms placed in regions where there is no pairing coherence would display only the electron component of their associated quasiparticles. The hole-like component, which appears only through pairing coherence, would not be visible. One can even imagine circumstances where ordinary quasiparticles found in metals, which are usually pure electron or pure hole, would lose their own coherence. For example, in the case of spin–charge separation the electron itself dissolves into two exotic particles, the 'spinon' and the 'holon'. In this event it is likely that neither an electron nor a hole component would be associated with the nickel atom.

Hudson *et al.*[1] provide a stunning demonstration of the effects of short-range disturbances in high-temperature superconductors. As methods for doping superconductors and modifying their surfaces improve, the possibilities for poking and prodding superconductors on the nanoscale grow even greater. ■

Michael E. Flatté is in the Department of Physics and Astronomy, University of Iowa, Iowa City, Iowa 52242, USA.
e-mail: michael_flatte@mailaps.org

1. Hudson, E. W. *et al. Nature* **411**, 920–924 (2001).
2. Flatté, M. E. & Byers, J. M. *Solid State Phys.* **52**, 137–228 (1999).
3. Yazdani, A., Jones, B. A., Lutz, C. P., Crommie, M. F. & Eigler, D. M. *Science* **275**, 1767–1770 (1997).
4. Pan, S. H. *et al. Nature* **403**, 746–750 (2000).

Neuroscience

Awareness of space

Michael S. A. Graziano

Damage to particular parts of the brain can cause spatial confusion and even eliminate awareness of areas of space around the body. The brain regions responsible for spatial awareness, however, are still under debate.

Certain types of brain damage can lead people to suffer from profound spatial disorientation and an inability to use spatial information to direct their movements — symptoms first described in detail near the beginning of the last century[1,2]. Some of the people who suffer from such damage, to the right posterior parietal lobe of the brain's cortex, show a phenomenon called hemispatial neglect[3], whereby they lose their awareness of the half of the space around them that lies opposite to the brain lesion. Someone with hemispatial neglect might shave only half of his face, dress just half of his body, or, when copying a picture, draw only one side of it.

On page 950 of this issue, Karnath and colleagues[4] revisit the topic of spatial neglect. They look at a set of patients with an especially pure form of the deficit, who lack some of the other symptoms that can occur together with hemispatial neglect after damage to the posterior part of the brain. The results threaten to overturn the century-old view that the parietal lobe (Fig. 1) is the region of the brain associated with spatial awareness.

The hypothesis that the parietal lobe is the key brain region for processing spatial information is based almost exclusively on studies of humans who have suffered damage to this part of the brain, often as the result of a stroke. Attempts to reproduce hemispatial neglect in monkeys by surgically damaging the parietal lobe have not been successful[5,6]. Such animals do have defects in processing somatosensory (tactile or heat) stimuli and in directing hand and eye move-

RAPID COMMUNICATIONS

PHYSICAL REVIEW B VOLUME 61, NUMBER 22 1 JUNE 2000-II

Quasiparticle resonant states as a probe of short-range electronic structure and Andreév coherence

Michael E. Flatté
Department of Physics and Astronomy, University of Iowa, Iowa City, Iowa 52242
(Received 31 January 2000)

The recently observed properties of quasiparticle resonant states near impurities on the surface of superconducting $Bi_2Sr_2CaCu_2O_{8+\delta}$ demonstrate that in-plane Andreév processes are either absent or phase incoherent. Analysis of the spectral and spatial details of the electronic structure near a Zn impurity also suggest an effective magnetic component of the impurity potential. Further experiments are proposed to clarify whether the effective moments of nearby impurities are correlated.

Over the past few years several authors have emphasized the wealth of information available from local probes of impurity properties in correlated electron systems, and particularly in superconductors whose homogeneous order parameters (OP's) are anisotropic in momentum.[1] A parallel improvement in scanning tunneling spectroscopy (STS) has allowed this vision to become a reality through direct observation of the local density of states (LDOS), first in niobium,[2] which has a momentum-independent OP, and this year in the high-temperature superconductor $Bi_2Sr_2CaCu_2O_{8+\delta}$ (BSCCO),[3–5] which has an anisotropic OP. The electronic structure of the BSCCO surface is much more complex than that of the niobium surface; there are local moments in the copper-oxygen planes and, under certain conditions, a pseudogap state. Recent work[6] has emphasized the role of the pseudogap state[7–9] in determining the properties of clean surfaces of high-temperature superconductors at temperatures near T_c, and STS and photoemission have directly demonstrated its existence on the surface of BSCCO. The pseudogap state is characterized by a single-particle gap of $d_{x^2-y^2}$ symmetry, but the Andreév processes one would expect in a superconducting state are (according to differences in mechanism) either absent or phase incoherent.

Here the STS measurements near impurities[3–5] will be shown to unambiguously demonstrate essentially complete suppression of Andreév processes in the vicinity of the impurity, even at very low temperatures. This low-temperature indication of a pseudogap implies its importance to the nature of the superconducting state and the operation of devices (such as Josephson junctions) with such materials. Indications of an effective magnetic component can also be seen in Ref. 5. Thus STS provides a direct probe of both the local Andreév (superconducting) coherence and the local magnetic properties on the BSCCO surface.

A brief review of the experimental results from Refs. 3–5 is in order. Theoretical predictions which have been confirmed include the presence of quasiparticle resonances near nonmagnetic impurities in anisotropic OP superconductors,[10] as well as the suppression of the gap feature near the impurity and the asymmetry of the resonance peak due to the energy dependence of the quasiparticle density of states.[11] The disagreements with previous theory, however, are striking. The most noticeable one is that the resonant state has only been detected on the *hole* side of the spectrum, both on the impurity site and *everywhere else around the impurity.* Whereas previous theories are consistent with an LDOS measured at the impurity which is entirely holelike, these same theories unambiguously predict the LDOS at nearest-neighbor states will be almost entirely electronlike. Indeed these theories predict the spatially integrated LDOS (or DOS) will be nearly particle-hole symmetric even though the LDOS at any particular site is not. A second unexpected element in the data is the presence of a second, much smaller, spectral peak on the hole side in Ref. 5. Whereas previous theories are consistent with two resonances at a single impurity, the spatially integrated amplitude of each resonance should be approximately the same, unlike what is seen in Ref. 5.

The above two issues are disagreements between the experimental and theoretical DOS, but there are also two significant disagreements in the LDOS. The resonance has a large amplitude at the impurity site, whereas calculations indicate that the largest amplitude in the LDOS should occur at the nearest-neighbor sites. Finally, the gap feature is seen on the impurity site, where it does not appear in calculations.[1]

The calculations here incorporate the pseudogap state into the evaluation of the differential conductance (dI/dV). After evaluating the LDOS for several impurity potential models, allowing for spatial extent and magnetic character in the potential, the impurities of Refs. 3–5 are found to be highly localized and the four discrepancies above can be reconciled. Finally, in the case of Ref. 5, a magnetic component to the effective Zn impurity potential is evident.[12]

The calculations of the LDOS are based on the Hamiltonian

$$H=\sum_{\langle ij\rangle,\sigma}\left[-t_{ij}c^{\dagger}_{i\sigma}c_{j\sigma}+\Delta_{ij}c^{\dagger}_{i\uparrow}c^{\dagger}_{j\downarrow}+\Delta^{*}_{ij}c_{j\downarrow}c_{i\uparrow}\right]$$

$$+\sum_{i}\left[(V_{0i}+V_{Si})c^{\dagger}_{i\uparrow}c_{i\uparrow}+(V_{0i}-V_{Si})c^{\dagger}_{i\downarrow}c_{i\downarrow}\right], \quad (1)$$

which includes a site-dependent potential which can be magnetic (V_S), nonmagnetic (V_0), or a combination of both. i and j label sites and σ labels spin. The homogeneous electronic structure, expressed as hopping matrix elements (t_{ij})

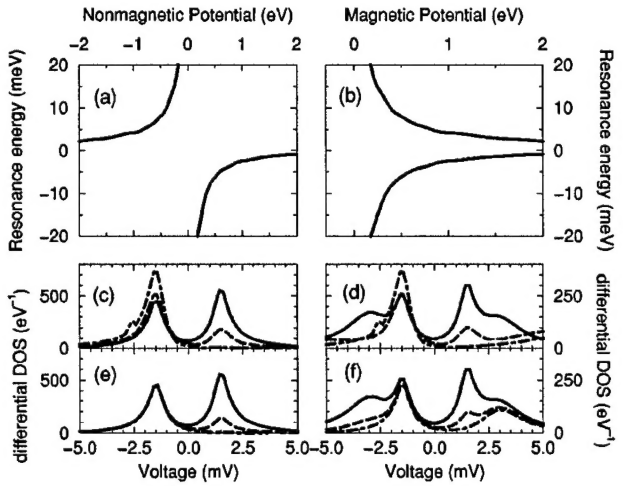

FIG. 1. Resonance energies for single-site (a) nonmagnetic and (b) magnetic impurity potentials. DOS for (c) nonmagnetic and (d) magnetic impurity potentials which produce a resonance at -1.5 mV. Solid, 40 meV superconducting gap, dashed, 25 meV superconducting, 40 meV total gap, dot-dashed, 40 meV nonsuperconducting gap. (e) and (f), same as (c) and (d) except the dashed line corresponds to partial and the dot-dashed line to no phase coherence in the 40 meV superconducting system.

for the first five nearest neighbors, is taken from a single-band parametrization of photoemission data.[13] Large variations in hopping matrix elements (>50 meV) produce results very much at odds with experiment, whereas smaller variations are mimicked by the site-dependent potential. Hence such changes will be ignored here. Only on-site and nearest-neighbor order parameters Δ_{ij} are nonzero, and the maximum OP on the Fermi surface, $\Delta_{max}=40$ meV.[14]

The electronic structure of the inhomogeneous system (including the impurity) is determined by direct numerical solution in real space of the Gor'kov equation (in Nambu form) for the inhomogeneous Green's function, $\mathbf{G}=\mathbf{g}+\mathbf{gVG}=(\mathbf{I}-\mathbf{gV})^{-1}\mathbf{g}$, within a real-space region around the impurity beyond which the potential is negligible.[1] The Δ_{ij}'s are found self-consistently in this process, for they determine the off-diagonal components of the potential $\mathbf{V}$. Spectra outside this real-space region are constructed according to the generalized $\mathbf{T}$-matrix equation: $\mathbf{G}=\mathbf{g}+\mathbf{gV}[\mathbf{I}-\mathbf{GV}]^{-1}\mathbf{g}$. Once $\mathbf{G}$ has been calculated throughout the region near the impurity, the LDOS and DOS are obtained from its imaginary part and the lattice Wannier functions. Then

$$\frac{dI(\mathbf{x};V)}{dV}=-\int d\omega\sum_{\sigma}\frac{1}{\pi}\left(\frac{\partial n_{STM}(\omega)}{\partial\omega}\right)|\phi_{\sigma}(\mathbf{x};i)|^2 \times \mathrm{Im}\,G_{\sigma}(i,i;\omega), \tag{2}$$

where $\phi_{\sigma}(\mathbf{x};i)$ is the overlap of the Wannier function at site i and spin σ with the STM tip at $\mathbf{x}$, and $n_{STM}(\omega)$ is the occupation function of the STM tip.[1] Resonances correspond to new peaks in the differential DOS (the difference between the inhomogeneous and homogeneous DOS); their energies are shown in Figs. 1(a) and 1(b) for magnetic and nonmagnetic single-site impurities.

If Andreév processes are suppressed, either by reduction in their amplitude or phase coherence, a resonance's DOS will become more electronlike or more holelike. Reduction of the amplitude of the homogeneous anomalous Green's function $f(i,j;\omega)$, due perhaps to a local antiferromagnetic (AF) order, decreases the mean-field coupling between electron and hole excitations. Note that this is very different from the fully electronlike or holelike character of the LDOS at the impurity, which originates from a vanishing $f(i,i;\omega)$ in the $d_{x^2-y^2}$ state. Figures 1(c) and 1(d) show the DOS of a resonance for three systems with a 40 meV $d_{x^2-y^2}$ gap: a fully superconducting gap (solid line), a gap with a 25 meV superconducting component (dashed line), and a pseudogap with no superconducting component (dot-dashed line). As the superconducting component is reduced, the electron-hole symmetry diminishes. The nonmagnetic potentials of Fig. 1(c) are chosen (1.375 eV, 1.000 eV, and 0.833 eV, respectively) so the resonance peak is at -1.5 mV (the same as Ref. 5). The magnetic potentials in Fig. 1(d) are the same as those in Fig. 1(c).

The reduction of the electronlike peak from phase decoherence is similar to the effect of amplitude suppression of $f(i,i;\omega)$. For a resonance at ω, the peak at $-\omega$ comes from terms with products of pairs of anomalous Green's functions. For a phase incoherent pseudogap state the expectation value of these pairs, and thus the amplitude of the electronlike peak, is diminished.[8] The effect of this is shown in Figs. 1(e) and 1(f) as a dashed line corresponding to partial (half) and a dot-dashed line corresponding to no phase coherence. The nonmagnetic potential is 1.375 eV in Fig. 1(e) and the magnetic potential is 1.375 eV in Fig. 1(f). Note that for the purely magnetic impurities even in the absence of Andreév coherence there is a peak on each side of zero energy.

For Refs. 3 and 5 there is no apparent electronlike component of the resonance in the DOS, thus local Andreév coherence is absent. In measurements of the LDOS near metal islands on BSCCO,[4] however, both holelike and electronlike peaks are apparent. This may indicate that the metal plays an important role in maintaining phase coherence at the surface, or that the metal overlayer is less disruptive to superconductivity than impurities in the plane. The presence of the in-plane Andreév processes, indicated by the electronlike peak, is essential to the operation of Josephson junctions.

The on-site LDOS of Ref. 5 is shown in Fig. 2(a). The second (holelike) peak is not as clearly evident in the results of Refs. 3 and 4, and thus may be peculiar either to the Zn impurity or to the impurity site in the BSCCO unit cell. Additional resonances around impurities can originate from additional orbital states around spatially extended potentials or from spin-splitting near magnetic potentials. Note that an effective magnetic potential could also originate from a nonmagnetic impurity potential placed in a spin-polarized host electronic structure.

Figures 2(a), 2(b), and 2(c) show the best fit of dI/dV to the data of Ref. 5 for phase incoherent Andreév processes and (i) a single-site nonmagnetic potential (1.375 eV), (ii) a nonmagnetic potential with onsite (0.360 eV) and nearest-neighbor (0.150 eV) values, and (iii) a mixed nonmagnetic and magnetic potential ($V_0=0.825$ eV, $V_S=0.550$ eV). Also shown is the best fit using (iv) a pseudogap with no superconducting component and a mixed potential ($V_0=0.543$

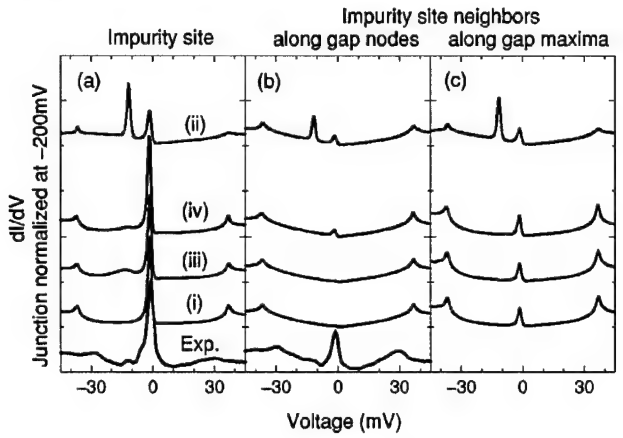

FIG. 2. dI/dV (a) on-site, (b) at the nearest neighbor along the gap nodes, and (c) along the gap maxima, for impurity and host models (i), (ii), (iii), and (iv). Data of Ref. 5 is also shown. The order of vertical offsets (introduced for clarity) of the curves in (b) and (c) is the same as in (a).

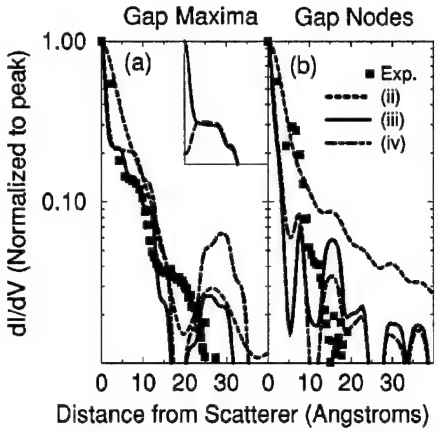

FIG. 3. dI/dV as a function of position along (a) the gap maxima and (b) the gap nodes. (ii) is dotted, (iii) is solid, and (iv) is dot-dashed. Shown in inset is the difference between dI/dV when junction normalization is (solid) and is not (dashed) taken into account.

eV, $V_S=0.290$ eV). The three panels show dI/dV (a) at the impurity site, (b) at the nearest-neighbor site along the gap nodes, and (c) along the gap maxima. Measurements of Ref. 5 for (a) and (b) are shown; (c) is not available.

The large size of the resonance on site and the simultaneous presence of the gap feature occur because of junction normalization (equal resistance at -200 mV) and the finite width of the $|\phi_\sigma|^2$ [modeled as Gaussians of range 0.8 Å, 3.8 Å, 0.8 Å, and 1.0 Å for (i)–(iv)]. The very small LDOS in this energy range at the impurity site causes the tip to approach closer to the surface and (1) enlarge the apparent size of the resonance on site, and (2) pick up the gap features from the nearest-neighbor sites. The relative size of the on-site resonance to the gap features is largely determined by the overlap of the nearest-neighbor Wannier functions with the tip when the tip is over the impurity site.

Judging from the comparison with experiment, (iii) and (iv) appear most in agreement. (i) does not have a second resonance, and whereas (ii) does show one in the proper location, its relative magnitude is incorrect. The smaller amplitude of the second resonance is obtained for (iii) and (iv) because the overlaps with the STM tip are spin dependent $[|\phi_\uparrow(\mathbf{x})|^2/|\phi_\downarrow(\mathbf{x})|^2 \sim 40]$. If the second peak were absent, either the impurity would lack magnetic character, or it would occur in less magnetic regions of the BSCCO unit cell. The remaining disagreement is in the amplitude of the resonance in Fig. 2(b), where (iv) is best, but still too small.

Figure 3 shows the amplitude of the resonance as a function of distance from the impurity along the gap maxima (a) and the gap nodes (b). The squares are the data from Ref. 5, whereas the solid line corresponds to (iii), the dotted line to (ii), and the dot-dashed line to (iv). The plot for (i) looks identical to that of (iii). The agreement of (iii) and (iv) are quite good along the maxima direction. The absence of a well-defined maximum at the nearest neighbor in (a), which was pointed out in Ref. 5, is due to the normalization procedure. An inset in Fig. 3 shows the difference between the junction normalized (solid) and unnormalized (dashed) dI/dV. The main discrepancy is with the amplitude of the signal along the node directions (b).

Figure 4 shows the dI/dV of the resonance for (iv); (iii) is similar. The differences between the Figs. 2–4 and the measurements of Ref. 5 may be due to errors in the homogeneous electronic structure of BSCCO used in the calculation, particularly the low-energy electronic structure which dominates the longer-range LDOS. These errors may be due to inaccuracies in the model for the electronic structure measured by photoemission,[13] or they may be due to the neglect of other collective effects on the surface. Another likely source of error is that the electronic structure model of the host is not spin dependent.

One of the possible mechanisms of a pseudogap is local AF order, such as occurs in a stripe.[9] The magnetic component apparent in the impurity potential suggests this origin as well. If two nearby impurity moments are aligned parallel, then the resonances associated with them will hybridize and split,[15] whereas if they are antiparallel the resonances will be degenerate. A careful examination of the dI/dV for two Zn atoms near each other on the surface may clarify whether there is local AF order.

The LDOS reported in Refs. 3–5 are best explained by the presence of a pseudogap state on the surface of BSCCO. The relative height of the electronlike and holelike reso-

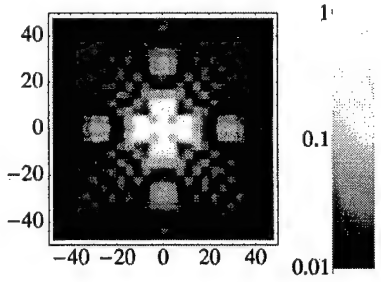

FIG. 4. Spatial structure of the dI/dV at the impurity resonance voltage (-1.5 mV) for (iv). Horizontal is parallel to the gap maxima directions.

nances in the DOS depends directly on the amplitude of local Andreév processes, and thus shows the degree of local superconducting coherence. This is of great practical interest, for the presence of these processes is essential to forming a proper Josephson junction across an interface. The information obtained about the superconducting state at the surface of BSCCO indicates the clear promise of future STM measurements near defects in other correlated electron systems.

I would like to thank J. C. Davis for discussions and for providing the data of Ref. 5. This work has been supported in part by ONR through Contract No. N00014-99-1-0313.

[1] See M. E. Flatté and J. M. Byers, in *Solid State Physics*, edited by H. Ehrenreich and F. Spaepen (Academic Press, New York, 1999), Vol. 52, and references therein.
[2] A. Yazdani *et al.*, Science **275**, 1767 (1997).
[3] E. W. Hudson *et al.*, Science **285**, 88 (1999).
[4] A. Yazdani *et al.*, Phys. Rev. Lett. **83**, 176 (1999).
[5] S. H. Pan *et al.*, Nature (London) **403**, 746 (2000).
[6] A. G. Loeser *et al.*, Science **273**, 325 (1996); Ch. Renner *et al.*, Phys. Rev. Lett. **80**, 149 (1998).
[7] G. V. M. Williams *et al.*, Phys. Rev. Lett. **78**, 721 (1997); G. Deutscher, Nature (London) **397**, 410 (1999).
[8] L. B. Ioffe and A. J. Millis, Science **285**, 1241 (1999).
[9] V. J. Emery and S. A. Kivelson, Nature (London) **374**, 434 (1995).
[10] M. I. Salkola, A. V. Balatsky, and D. J. Scalapino, Phys. Rev. Lett. **77**, 1841 (1996).
[11] M. E. Flatté and J. M. Byers, Phys. Rev. Lett. **80**, 4546 (1998).
[12] This has been seen in YBCO [A. V. Mahajan *et al.*, Phys. Rev. Lett. **72**, 3100 (1994)].
[13] M. R. Norman, M. Randeria, H. Ding, and J. C. Campuzano, Phys. Rev. B **52**, 615 (1995).
[14] Measured gap features at the surface vary from sample to sample as well as from point to point on the same sample. 40 meV is a typical location for the gap feature.
[15] M. E. Flatté and D. E. Reynolds, Phys. Rev. B **61**, 14 810 (2000).

Local spectrum of a superconductor as a probe of interactions between magnetic impurities

Michael E. Flatté and David E. Reynolds*
Department of Physics and Astronomy, University of Iowa, Iowa City, Iowa 52242
(Received 2 February 2000)

Qualitative differences in the spectrum of a superconductor near magnetic impurity pairs with moments aligned parallel and antiparallel are derived. A proposal is made for a nonmagnetic scanning tunneling spectroscopy of magnetic impurity interactions based on these differences. Near parallel impurity pairs the midgap localized spin-polarized states associated with each impurity hybridize and form bonding and antibonding molecular states with different energies. For antiparallel impurity moments the states do not hybridize; they are degenerate.

The relative orientation of the moments of two magnetic impurities embedded nearby in a metallic nonmagnetic host will depend on the significance of several electronic correlation effects, such as direct exchange, double exchange, superexchange, and Ruderman-Kittel-Kasuya-Yosida (RKKY) interactions. Each of these effects produces characteristic moment orientation; e.g., the RKKY interactions can align moments either parallel or antiparallel depending on the impurity separation. Reliable experimental measurements of the moment orientation as a function of impurity separation could identify the origin of magnetism in alloys of technological significance, such as the metallic ferromagnetic semiconductor GaMnAs,[1] which may eventually play a crucial role in semiconductor-based magnetoelectronics.[2] Such measurements should also clarify the interplay between metallic and magnetic behavior in layered oxides, such as the high-temperature superconductors. In this work we propose, based on theoretical calculations, a robust experimental technique for the systematic and unambiguous experimental determination of moment alignment as a function of impurity separation.

We demonstrate that in an electronic system with a gap there is a fundamental difference between the electronic states localized around parallel and antiparallel impurity moments. Around parallel impurity moments there are midgap *molecular* states (similar to bonding and antibonding states in a diatomic molecule). Around antiparallel impurity moments the states remain more *atomiclike* and are degenerate. This qualitative difference in the spectrum of an impurity pair provides a robust technique of determining the impurity-impurity interaction via *nonmagnetic* scanning tunneling spectroscopy (STS). The essential condition for practical application of this technique will be whether the splitting of the states around parallel impurity moments is large enough to be observed spectroscopically.

The gapped system we consider in detail is the superconductor $NbSe_2$, which is chosen for its extremely favorable surface properties for STS and for its quasi-two-dimensional electronic structure. STS has already been used to examine the localized states which form near isolated magnetic impurities on the surface of superconducting niobium.[3,4] We have calculated the energies and spatial structure of the electronic states near impurity pairs in $NbSe_2$ essentially exactly within mean-field theory. These calculations indicate that the size of the splitting of states around parallel impurity moments in $NbSe_2$ is measurable—they are split by a sizable percentage of the energy gap even for impurity moment separations of order 30 Å.

A nonmagnetic spectroscopy of magnetic impurity interactions is also plausible in a much wider range of materials. The localized spin-polarized states upon which the technique is based occur near magnetic impurities in most systems where there is a gap in the single-particle density of states at the chemical potential, whether or not the gap originates from superconductivity. Even when there is no true gap, if the density of states is substantially reduced at the chemical potential sharp resonances similar to the localized states will form (this has been predicted and recently observed for d-wave superconductors).[5–7] Resonances around parallel and antiparallel impurity pairs show similar qualitative features to localized states.

If the energy scales of moment formation and interaction are much greater than those responsible for creating the gap it is also possible to infer the impurity interaction within a material in its high-temperature metallic phase from spectroscopic measurements on the same material in a low-temperature superconducting phase. In this the STS procedure is similar to traditional "superconducting spectroscopy,"[8] where the dependence on impurity concentration of the superconducting transition temperature T_c or the specific-heat discontinuity at T_c is used to determine the presence and rough magnitude of a single-impurity moment. However, whereas single-impurity information can often be extracted from such measurements in the dilute limit, pairwise impurity interactions are much more difficult to infer from macroscopic properties such as T_c which depend on an ensemble of local configurations.

We note that the technique described here is remarkably noninvasive compared to alternate methods. The use of a magnetic tip to probe the magnetic properties of a sample[9] may distort the natural surface orientation of moments. An alternative nonmagnetic STS technique that has been proposed, which involves a superconducting tip[10] in a Tedrow-Meservey geometry,[11] requires either an external or surface-induced magnetic field to spin-split the superconducting density of states (DOS) of the tip. Finally, the use of spin-polarized tunneling from a GaAs tip relies on a fixed orientation of the magnetic structure on the surface relative to that of the optically generated spin-polarized population in the tip.[12]

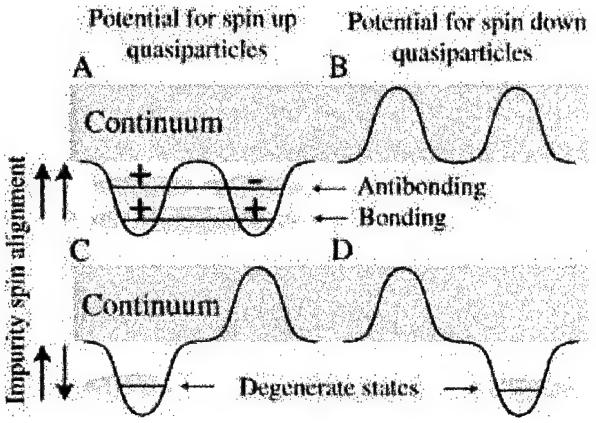

FIG. 1. (Color) Schematic of the potential for spin-up [left side, (A) and (C)] and spin-down [right-side, (B) and (D)] quasiparticles in the presence of parallel impurity spins [top row, (A) and (B)] and antiparallel impurity spins [bottom row, (C) and (D)]. For parallel impurity spins there are two localized states of spin-up quasiparticles which differ in energy, similar to the bonding and antibonding states of a diatomic molecule. There are no localized states of spin-down quasiparticles. For antiparallel impurity spins there is one spin-down quasiparticle localized state, as well as one of spin up, and the two are degenerate.

To understand the origin of the nondegeneracy of states around parallel moments and the degeneracy of states around antiparallel moments consider a heuristic picture of the two-impurity system in an isotropic-gap superconductor. For parallel alignment of the impurity moments only quasiparticles of one spin direction (assumed to be spin up) will be attracted to the impurity pair. Any localized state will thus be spin up. If the two impurities are close their two spin-up atomiclike states will hybridize and split into molecular states just as atomic levels are split into bonding and antibonding states in a diatomic molecule. Thus there will be two nondegenerate states apparent in the spectrum. This is shown schematically in the top section of Fig. 1, where the potential for spin-up quasiparticles is shown on the left [Fig. 1(A)] and for spin-down quasiparticles is shown on the right [Fig. 1(B)]. The potential for spin-down quasiparticles is everywhere repulsive, so no spin-down localized states will form.

The situation for antiparallel aligned spins, shown on the bottom of Fig. 1, is quite different. The effect of the second impurity on the state around the first is *repulsive* and so does not change the state energy much unless the impurities are very close. Furthermore the Hamiltonian has a new symmetry in this case: it is unchanged under the operation which both flips the quasiparticle spin and inverts space through the point midway between the two impurities. This operation changes the potential of Fig. 1(C) into that of Fig. 1(D). Thus instead of split states we find two degenerate atomiclike states of opposite spin, localized around each of the two impurities.

Detailed results for $NbSe_2$ are obtained by solving the following lattice-site mean-field Hamiltonian self-consistently:

$$H=-\sum_{\langle ij\rangle,\sigma} t_{ij}c_{i\sigma}^{\dagger}c_{j\sigma}+\sum_{i}\left[\Delta_i c_{i\uparrow}^{\dagger}c_{i\downarrow}^{\dagger}+\Delta_i^{*}c_{i\downarrow}c_{i\uparrow}\right] + V_{S1}(c_{1\uparrow}^{\dagger}c_{1\uparrow}-c_{1\downarrow}^{\dagger}c_{1\downarrow})+V_{S2}(c_{2\uparrow}^{\dagger}c_{2\uparrow}-c_{2\downarrow}^{\dagger}c_{2\downarrow}), \quad (1)$$

where $c_{i\sigma}^{\dagger}$ and $c_{i\sigma}$ create and annihilate an electron at lattice site i with spin σ. The impurities reside at lattice sites 1 and 2, the t_{ij} are the hopping matrix elements, and the Δ_i are the values of the superconducting order parameter. $NbSe_2$ has a triangular lattice, and the normal-state band structure can be

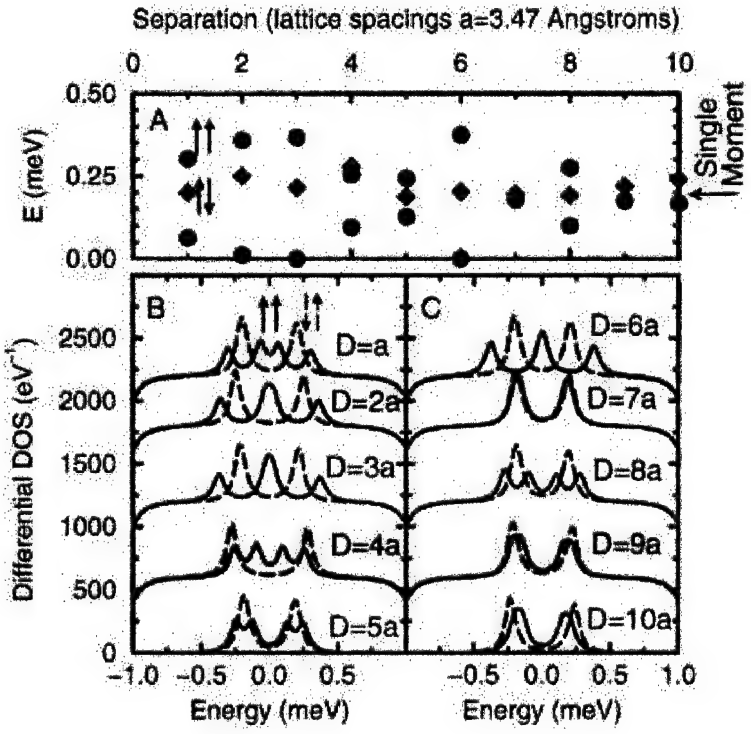

FIG. 2. (Color) (A) Energies of localized states as a function of impurity separation near parallel impurity spins (red) and antiparallel impurity spins (black). The energy is in meV and impurity separation in nearest-neighbor in-plane lattice constants (3.47 Å). (B) Differential density of states (DOS) for parallel impurity pairs (solid lines) and antiparallel impurity pairs (dashed lines) for impurity separations from one to five lattice spacings. (C) Same as (B), except for six to ten lattice spacings.

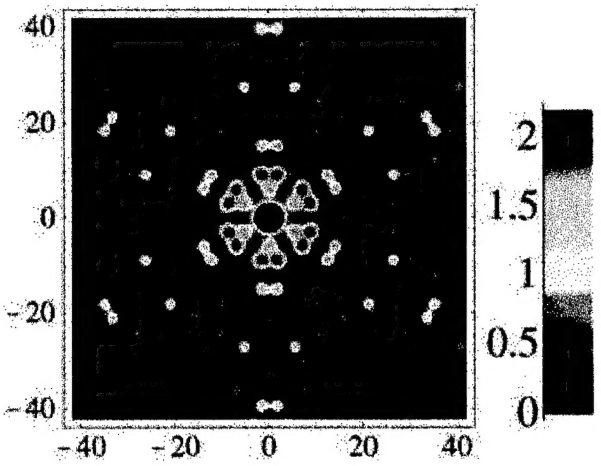

FIG. 3. (Color) Spatial structure of the holelike local density of states (LDOS) around a single impurity in the surface layer of $NbSe_2$. Nearest-neighbor in-plane separation on the triangular lattice is 3.47 Å. The units of the color scale are eV^{-1}.

modeled with an on-site energy of −0.1 eV and with nearest-neighbor and next-nearest-neighbor hopping matrix elements of −0.125 eV. These are determined from a tight-binding fit[13] to *ab initio* calculations of the electronic structure.[14] The superconducting pairing interaction is modeled with an on-site attractive potential which yields the experimental order parameter $\Delta = 1$ meV. The inhomogeneous order parameter Δ_i is determined self-consistently from the distorted electronic structure in the vicinity of the impurities. We consider equivalent parallel ($V_{S1} = V_{S2}$) or antiparallel ($V_{S1} = -V_{S2}$) impurity moments.

This model assumes the impurity spins behave as classical spins (see Refs. 3, 4, and 6). Classical spin behavior has been seen, for example, for Mn and Gd impurities on the surface of niobium.[3] The electronic structure in this model, including quasiparticle state energies and spatial structure, can be found rapidly and accurately by inverting the Gor'kov equation in a restricted real-space region including the two impurities, as described in Ref. 6. Measurements of the spatial structure of these states and of the values of the splitting

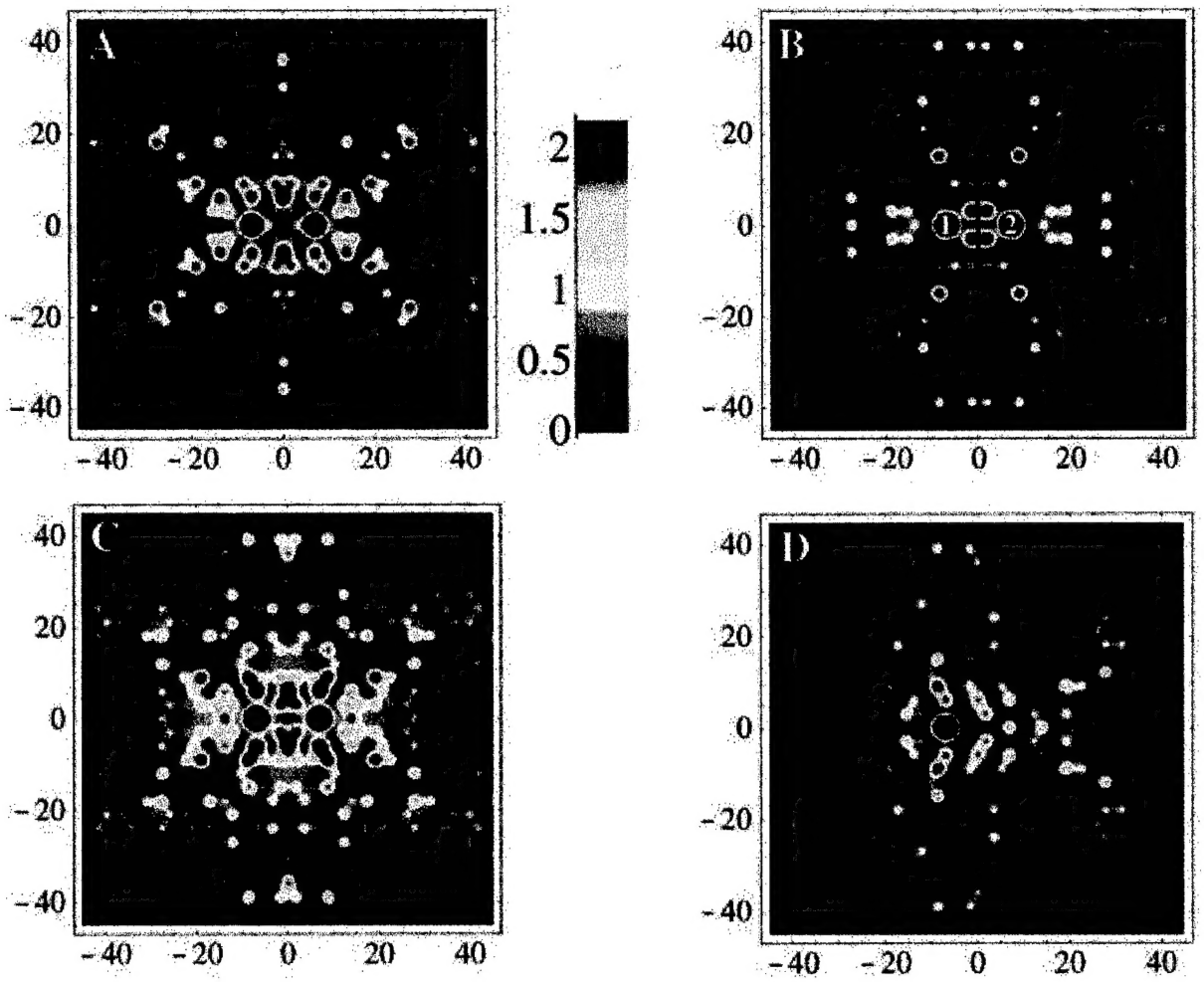

FIG. 4. (Color) LDOS around a parallel impurity pair at (A) the energy corresponding to the bonding state (−0.10 meV), and (B) the energy corresponding to the antibonding state (−0.26 meV). The impurities are at the same sites in each of (A)–(D), labeled 1 and 2 in (B). The mirror plane between the impurities is indicated by the red line in (B); there is no LDOS for the antibonding state in (B) along this plane, while there is for the bonding state (A). (C) LDOS around an antiparallel impurity pair at the energy of localized states (−0.28 meV). (D) spin-resolved LDOS at the same energy as (C) showing the predominance of LDOS around the impurity on the left. The units of the color scale are eV^{-1}.

between states can serve as a sensitive test of the model of the electronic structure of this material and of the impurity potential for a given atom.

Figure 2(A) shows the energies of the localized states in $NbSe_2$ for parallel spins (red) and antiparallel spins (black) for a sequence of impurity spacings which are multiples of the in-plane nearest-neighbor vector of the $NbSe_2$ lattice. The splitting of the bonding and antibonding states oscillates over a distance scale comparable to the Fermi wavelength of $NbSe_2$ along this direction. The splitting is proportional to the probability of a quasiparticle at one impurity propagating to the other, which is a measure of the coupling of the two atomiclike states. At large distances state energies for parallel and antiparallel moments approach the single impurity state energy, indicated on the right side of Fig. 2(A). Figure 2(B) and (C) shows the spatially integrated change in density of states due to the impurity pair for these impurity separations. The DOS of a quasiparticle of energy E in a superconductor has an electron component at energy E and a hole component at energy $-E$, so a single state will produce two peaks in the DOS unless it is closer to $E=0$ than the linewidth. That linewidth is determined by thermal broadening in the metallic probe tip, which for these plots is assumed to be 0.05 meV=0.6 K. The gap in the homogeneous DOS extends from -1 meV to 1 meV in $NbSe_2$, so the variation in state energies is a substantial fraction of this gap. The clear distinction between parallel and antiparallel impurity moments in the DOS is only limited by the linewidth of the states.

A tunneling measurement of the DOS using a broad-area contact would yield the spectrum of an ensemble of impurity separations, hence STS (which measures the local DOS, or LDOS) is the ideal method for examining a single configuration of impurities. Before describing the distinct spatial differences in LDOS measurements between parallel and antiparallel alignments of impurity pairs we show the single impurity result in Fig. 3. The spatial structure of the electron and hole components of the LDOS are independently measurable by STS and can be quite different in detail. In this work we will show only the spatial structure of the hole component—similar gross structure is seen in the electronlike LDOS. Figure 3 shows the sixfold symmetric LDOS for $NbSe_2$ for $V_S=200$ meV at an energy of -0.19 meV. The units are angstroms and the nearest-neighbor spacing is 3.47 Å.

The details of the spatial structure can be traced directly to the normal-state electronic structure of $NbSe_2$.[6] We note that the local hopping matrix elements and the local nonmagnetic potential will differ near the impurity atoms. We find that moderate changes in these quantities do not significantly change the magnitude of the splitting of the even and odd parity states. This relative insensitivity occurs because the splitting is largely dependent on the amplitude for a quasiparticle to propagate from one impurity site to the other. Careful comparison of a measured LDOS and Fig. 3 would allow the determination of any changes in the local hopping or the nonmagnetic potential.

Plots of the LDOS for two impurities in $NbSe_2$ separated by four lattice spacings (13.88 Å) are shown in Fig. 4(A)–(D). They demonstrate via their spatial structure the qualitative differences among different types of molecular states possible around an impurity pair. Figure 4(A) is the bonding state (energy -0.10 meV) and Fig. 4(B) shows the antibonding state (-0.26 meV). The impurities are at the same sites in each of Fig. 4(A)–(D), labeled 1 and 2 in Fig. 4(B). As expected from the symmetry of these states, the antibonding state has a nodal line along the mirror plane (indicated in red) between the two impurities. No such nodal line occurs in Fig. 4(A)—in contrast the state is enhanced along the mirror plane.

The nonmagnetic STS probe cannot resolve the spin direction of the electronic states around the impurities, so around antiparallel impurity moments it detects both states. The sum of the LDOS for the two atomiclike states is symmetric around the mirror plane. Figure 4(C) is the LDOS at the energy for the two degenerate states around antiparallel impurity spins (-0.28 meV). The states are much more diffuse than the bonding state in Fig. 4(A) due to the repulsive nature of one impurity. Figure 4(D) shows the spin-resolved LDOS (which is more difficult to access experimentally), showing the LDOS of holes with the spin direction attracted to the impurity on the left. The spin-resolved LDOS at the impurity on the left is two orders of magnitude greater than at the impurity on the right. Thus the individual localized states are quite atomiclike.

We have assumed throughout that the impurity moments are locked either parallel or antiparallel. If the alignment is intermediate between the two cases then the spectrum shows nondegenerate states split less than in the parallel case. If there is some flipping of moments between parallel and antiparallel alignment on a timescale longer than the time required for the quasiparticle states to realign with the moments then the spectrum would be a linear superposition of the antiparallel and parallel spectra. If this is an activated process, this energy of activation of moment flipping could be easily distinguished by examining the temperature dependence of the spectrum.

This work describes a robust technique for determining the alignment of two impurity moments in a gapped system. The details of the expected results around magnetic impurities in the quasi-two-dimensional superconductor $NbSe_2$ have been calculated. Energies and spatial structure of bonding and antibonding states around parallel moments, and of localized atomiclike states around antiparallel moments, indicate that the two cases should be distinguishable with nonmagnetic scanning tunneling spectroscopy. This technique should be broadly applicable to a wide range of correlated electronic systems.

We would like to acknowledge the Office of Naval Research Grant Nos. N00014-96-1-1012 and N00014-99-1-0313. This research was supported in part by the National Science Foundation under Grant No. PHY94-07194.

*Present address: Department of Physics, University of California, Santa Barbara, California 93106.

[1] B. Beschoten *et al.*, Phys. Rev. Lett. **83**, 3073 (1999).
[2] H. Ohno, Science **281**, 951 (1998).
[3] A. Yazdani, B. A. Jones, C. P. Lutz, M. F. Crommie, and D. M. Eigler, Science **275**, 1767 (1997).
[4] H. Shiba, Prog. Theor. Phys. **40**, 435 (1968).
[5] M. I. Salkola, A. V. Balatsky, and D. J. Scalapino, Phys. Rev. Lett. **77**, 1841 (1996).
[6] M. E. Flatté and J. M. Byers, in *Solid State Physics*, edited by H. Ehrenreich and F. Spaepen (Academic Press, New York, 1999), Vol. 52.
[7] E. W. Hudson *et al.*, Science **285**, 88 (1999); A. Yazdani, C. M. Howald, C. P. Lutz, A. Kapitulnik, and D. M. Eigler, Phys. Rev. Lett. **83**, 176 (1999); S. H. Pan *et al.*, Nature (London) **403**, 746 (2000).
[8] M. B. Maple, in *Moment Formation in Solids*, edited by W. J. L. Buyers (Plenum, New York, 1984), p. 1.
[9] M. Bode, M. Getzlaff, and R. Wiesendanger, Phys. Rev. Lett. **81**, 4256 (1998).
[10] S. H. Pan, E. W. Hudson, and J. C. Davis, Appl. Phys. Lett. **73**, 2992 (1998).
[11] R. Meservey, Phys. Scr. **38**, 272 (1988).
[12] S. F. Alvarado and P. Renaud, Phys. Rev. Lett. **68**, 1387 (1992); S. F. Alvarado, *ibid.* **75**, 513 (1995).
[13] W. Sacks, D. Roditchev, and J. Klein, Phys. Rev. B **57**, 13 118 (1998).
[14] A. Kikuchi and M. Tsukada, Surf. Sci. **326**, 195 (1995).

REPORT DOCUMENTATION PAGE

Form Approved
OMB No. 0704-0188

1. REPORT DATE *(DD-MM-YYYY)*	2. REPORT DATE	3. DATES COVERED *(From - To)*
08-10-2001	October 8. 2001	Performance (7/1/00-6/30/01)

4. TITLE AND SUBTITLE

Nanoscale coherence near defects:
Superconductivity, spin ordering and their coexistence.

5a. CONTRACT NUMBER

5b. GRANT NUMBER
N00014-99-1-0313

5c. PROGRAM ELEMENT NUMBER

6. AUTHOR(S)

Flatté, Michael E.

5d. PROJECT NUMBER

5e. TASK NUMBER

5f. WORK UNIT NUMBER

7. PERFORMING ORGANIZATION NAME(S) AND ADDRESS(ES)

The University of Iowa
Iowa City, IA 52242

8. PERFORMING ORGANIZATION REPORT NUMBER

9. SPONSORING/MONITORING AGENCY NAME(S) AND ADDRESS(ES)

Office of Naval Research
Ballston Centre Tower One
800 North Quincy Street
Arlington, VA 22217-5660

10. SPONSOR/MONITOR'S ACRONYM(S)
ONR

11. SPONSORING/MONITORING AGENCY REPORT NUMBER

12. DISTRIBUTION AVAILABILITY STATEMENT

APPROVED FOR PUBLIC RELEASE

13. SUPPLEMENTARY NOTES

14. ABSTRACT

This is a report of progress in theoretical calculations of the influence of impurities on tunneling spectroscopy in high-temperature superconductors. The calculations have been improved by the addition of energy-dependent linewidths and bilayer splitting. Notable results include the use of Ni as a local probe for superconductivity, the lack of splitting from the bilayer of the quasiparticle resonances, and the independence of low-energy quasiparticles from bilayer splitting. Preliminary theoretical views of noise in tunnel junctions have been presented as well.

15. SUBJECT TERMS

Superconductivity, impurities, noise, tunnel junctions, dielectric loss.

16. SECURITY CLASSIFICATION OF:			17. LIMITATION OF ABSTRACT	18. NUMBER OF PAGES	19a. NAME OF RESPONSIBLE PERSON
a. REPORT	b. ABSTRACT	c. THIS PAGE		18	Michael E. Flatté
					19b. TELEPONE NUMBER *(Include area code)* 1-319-335-0201